PtCo/C cathode catalyst for improved durability in PEMFCs

Ping Yu [*], Marianne Pemberton, Paul Plasse

UTC Fuel Cells LLC, 195 Governor's Highway, South Windsor, CT 06074, USA

Abstract

A major challenge to the application of Pt–transition metal alloys in PEMFCs is the stability of the Pt alloy. This work intends to evaluate the durability of PtCo/C cathode catalyst in a dynamic fuel cell environment with continuous water fluxing on the cathode. A potential cycling test between 0.87 and 1.2 V versus RHE was applied to the system to illustrate how cobalt or platinum dissolution might affect the cell performance. The results indicate that cobalt dissolution neither detrimentally reduces the cell voltage nor dramatically affects the membrane conductance. Cell performance enhancement by PtCo/C over Pt/C catalyst has been sustained over 2400 cycles and the overall performance loss of the PtCo/C membrane electrode assemblies (MEAs) was less than that of the Pt/C MEA. Potential cycle testing has been shown to accelerate cobalt dissolution as indicated in a substantial loss of catalyst activity in the 1st 400 potential cycles.
© 2005 Elsevier B.V. All rights reserved.

Keywords: PEM fuel cells; PtCo alloy; Cathode catalyst; Metal dissolution; Durability

1. Introduction

Platinum alloys as cathode catalysts have attracted wide attention as a candidate to achieve high performance, to increase in power density, and to reduce a component cost of PEMFCs [1,2]. Extensive research has been conducted in areas of new alloy development and understanding of mechanisms of electrochemical oxygen reduction reaction (ORR) [1–11]. However, a relatively small number of publications are related to the durability of Pt alloys in the fuel cell environment [13–17]. One concern with Pt alloys in fuel cells is dissolution of transition metal. Pourbaix diagrams [18] indicate that most metals such as Co, Cr, Fe, Ni, Mn, Cu, and V are soluble at a potential between 0.3 and 1 V versus SHE and at pH of around 0. The value of 0 is a typical pH of the medium to which Pt alloys are subjected to with perfluorosulfonic acid (PFSA) as an electrolyte in PEMFCs. The dissolution of transition metals in Pt alloys could result in a decrease of catalyst

activity for ORR if the catalyst activity is enhanced by the addition of transition metal in the platinum crystal structure [3]. Metal cations from the dissolution could easily exchange with a proton of PFSA membrane/ionomer because of a stronger affinity of metal cations than proton with the sulfonic group [15]. Exchange of metal cations with the sulfonic group might affect the performance of the fuel cell as categorized to three aspects [15]: (i) decreasing ionomer/membrane conductivity, as an example given by Okada [15], the ionic conductivity of Nafion decreases by 50% when 20–25% ionomer proton sites were exchanged with Cu^{2+} upon soaking the membrane in a liquid copper salt solution; (ii) reducing water content and dehydrating membranes; Okada et al. reported [16] that the water content (λ) in Nafion 117 decreased from 22 to 20 as the iron ion exchanged increased from 0 to 75%; (iii) suppressing oxygen reduction kinetics by a decrease of oxygen concentration or oxygen diffusion coefficient in ionomer film. It was shown by Okada et al. [19] that the activity for ORR decreased by ca. 22% when a Nafion film was exchanged with Ni^{2+} to about a 1–10% level. All three effects obviously could reflect on the cell voltage, i.e., could lead to a performance degradation of the PEMFCs and could be detrimental to the commercialization of longer lifetime PEMFC

* Corresponding author. Present address: Hamilton Sunstrand Space Systems International M/S 1A-2-W66, 1 Hamilton Road, Windsor Locks, CT 06096-1011, USA. Tel.: +1 860 654 6492; fax: +1 860 660 9011.

E-mail address: ping.yu@hs.utc.com (P. Yu).

cell stacks. Investigation of this issue and developing a mitigation strategy is essential to ensure a successful application of Pt alloy catalysts in PEM cell stacks.

It is noted that most metal contamination tests illustrated in the literatures were conducted in an ex situ fuel cell environment with a static mode [15–17,19]. In that case, a piece of membrane was immersed in an aqueous solution of a known cation concentration for a period of time and there was an accumulated effect on membrane properties because no excess water was introduced to the membrane surface for removing cation contaminants. This is different from a fuel cell operation mode in which water continuously generated on the cathode by an oxygen reduction fluxes to the catalyst layer, which will carry metal cations to exit a cell stack. If the flow rate is high enough on the cathode, a significant portion of cation could be removed from the cell stack without much exchange to the membrane/ionomer. In this case, membrane conductance will not be detrimentally altered as long as water continuously fluxes out and cell performances will not be dramatically affected accordingly. In this case, cell stack design and water management are critical in excluding metal contaminants before the detrimental effect takes place. Therefore, it is essential to investigate the dynamic effects of metal dissolution on cell performance under fuel cell operation conditions and in a real design configuration.

This work intends to evaluate the stability of PtCo/C catalysts under PEMFC operating conditions and to investigate possible influences of cobalt or platinum dissolution on oxygen reduction kinetics, membrane conductance, and mass transport resistance.

2. Experimental

PtCo/C catalyst supported on carbon with platinum loading of approximately 50 wt% was prepared with a wet chemistry procedure [21]. In brief, 2 g Ketjen Black EC-300J (Akzo Nobel) powder as a carbon support was dispersed in deionized (DI) water, 5.75 g chloroplatinic acid ($H_2PtCl_6 \cdot 6H_2O$, Alfa Aesar) as a platinum salt was added to the dispersion and 5 ml 37% formaldehyde (HCOH, Aldrich) as a reducing agent was introduced afterward. In order to control the platinum particle size [20], carbon monoxide (20% CO in N_2, Praxair) was flowed to the dispersion when Pt was deposited on carbon. After being filtered, washed with DI water and dried in a vacuum oven at 90 °C, the Pt/C catalyst precursor was redispersed in 1.03 g of cobalt nitrate solution ($Co(NO_3)_2 \cdot 6H_2O$, Fisher), and the mixture was dried at 90 °C. The dried mixture of Pt/C and $Co(NO_3)_2$ was then heat-treated at 900 °C for 1 h under a continuous flow of Ar gas (99.9%, Praxair). This step was to reduce Co^{2+} ion to Co metal by carbothermal reduction [21] and to alloy the Pt and Co metals. The blackish powder produced after the heat treatment was the PtCo/C catalyst used for all the forthcoming durability evaluations in this communication. For comparison purpose, platinum catalyst (TEC10E50E) supported on

carbon prepared by Tanaka Kikinzoku Kogyo K.K. (TKK, Japan) was used as a baseline. Platinum metal loading of the Pt/C catalyst is 48.4 wt%. Pt/C in the reminder of the manuscript refers to the commercial 48.4 wt% Pt/C catalyst from TKK.

Membrane electrode assemblies (MEAs) used in this study were prepared with the PtCo/C or Pt/C catalyst for the cathode and Pt/C catalyst for the anode. Platinum loading was 0.4 mg cm^{-2} on each electrode layer of the MEA. Nafion 112 film with a thickness of 50 μm (DuPont) was used as a membrane and Toray H065 carbon paper (Toray Industries, Japan) with a thickness of 175 μm was used as a gas diffusion layer. MEAs were fabricated by coating a catalyst ink mixture of 30 wt% Nafion (5 wt% Nafion solution, Aldrich) and 70 wt% catalyst on each side of membrane. A MEA was sandwiched between two gas diffusion layers to form a cell assembly. The active area of the MEA was 25 cm^2. Cell operation conditions were 65 °C and 101 kPa (absolute). Both hydrogen and air (or oxygen) reactants were internally humidified in a cell configuration, where a porous water transport plate was employed as a bipolar plate [22,23] and a full humidity of reactants is assumed.

After initial performance evaluation on the MEAs, a potential cycling test was conducted to investigate possible effects of metal dissolution on cell performances. This was done by subjecting the cathode side of the cell to a potential cycling between 0.87 and 1.2 V versus RHE. A potential square wave generated by a Potentiostat/Galvanostat Model 273A (EG&G Princeton Applied Research) was used with a time step of 30 s at each potential. The potential limit of 0.87 V versus RHE was chosen to mimic the cathode potential under H_2/air operation condition and at a low current density, while the potential limit of 1.2 V versus RHE was selected to simulate the cathode potential at open circuit condition of fuel cells with air flowing to both anode and cathode. Hydrogen fuel was fed to the anode and nitrogen to the cathode during testing. The purpose of this test was to force a considerable dissolution of metals from the alloy including both platinum and cobalt and then to investigate possible effects of metal dissolution on cell performances. Cell diagnosis such as H_2/air and H_2/O_2 performances were periodically evaluated after every 400 potential cycles. Membrane resistance and cathode electrochemical area (ECA) of platinum were evaluated at the same time. In total, 2400 cycles were conducted in each cell. The flow rate of hydrogen, air and oxygen was fixed to be 500, 3000, and 1000 cm^3 min^{-1}, respectively, during performance evaluation. Cyclic voltammograms for ECA determination were taken with 4% H_2 balance with N_2 on the anode and DI water on the cathode at 65 °C and all data points were collected using CorrWare Software (Scribner Associates Inc.). A typical ECA was determined by calculating the hydrogen adsorption charge on the platinum surface and dividing the charge over a value of 210 C cm^{-2} assuming a monolayer adsorption of hydrogen atom on platinum surface.

MEAs before and after cell testing and catalysts were characterized to determine alloy physical properties. Anal-

ysis on metal element distribution in cross-section of MEA was performed with JEOL 8900 Electron Probe Analyzer. X-ray diffraction (XRD) analysis was conducted with Rigaku RU-200B unit using a rotating Cu anode to investigate variation of catalyst crystal structure. Transmission electron microscope (TEM) with Philips FEI CM2000 unit was used to overview the surface morphology of catalyst and to determine the particle distribution. Inductively couple plasma (ICP) analysis with a model TJA was conducted to determine catalyst composition and dissolved metal concentration in a solution.

3. Results and discussions

3.1. PtCo/C and Pt/C catalyst characterization

Platinum crystal structure and particle distribution of PtCo/C catalyst powder were characterized with XRD and

Table 1
Properties of PtCo and Pt catalysts determined by XRD

Catalyst	Lattice parameter (nm)	Crystal size (nm)	Composition (wt%)	
			Pt	Co
Pt/C	0.392	2.50	48.4	
PtCo/C	0.382	4.55	46.8	5.2

TEM and the results are given in Figs. 1 and 2, respectively. Pt/C catalyst was evaluated as well for comparison. As observed in Fig. 1, the diffraction pattern of PtCo/C is similar to Pt/C catalyst in terms of peak position and peaks of Pt/C catalyst appears wider than those of PtCo/C catalyst. It is noted that no individual peaks of cobalt were detected, which indicates cobalt might be fully incorporated into the Pt crystal to form an alloy since the ICP data confirms an existence of cobalt in the alloy. Lattice parameter and particle size of the PtCo/C catalyst were calculated from the patterns and are summarized in Table 1. As shown in Table 1, the average crystal size of Pt in PtCo/C catalyst was 4.55 nm, which was
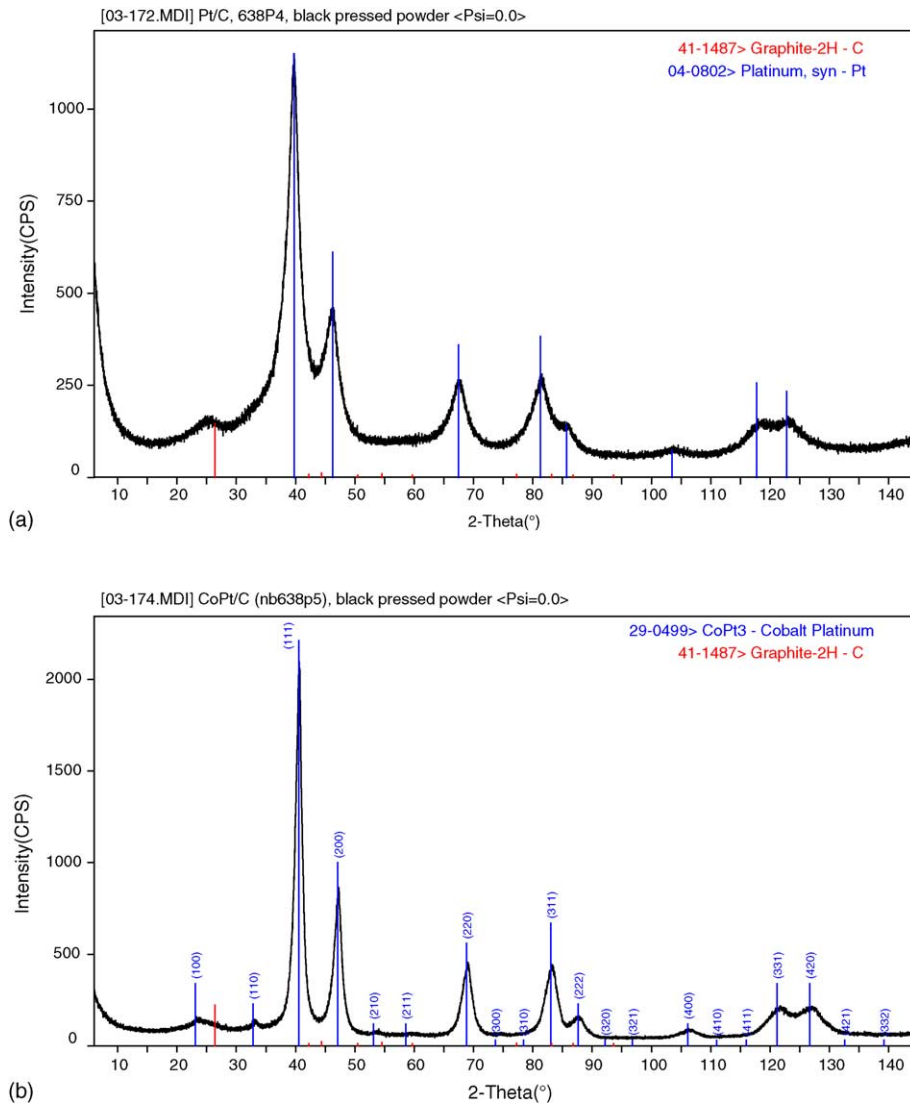

Fig. 1. XRD patterns of (a) Pt/C catalyst (TKK catalyst) and (b) PtCo/C alloy catalyst.

greater than Pt/C catalyst of 2.5 nm. The lattice parameter of platinum in PtCo/C catalyst was 0.382 nm, which is smaller than Pt/C catalyst of 0.392 nm. The decrease in lattice parameter of PtCo/C alloy indicates that addition of cobalt in the Pt crystal reduced the spacing of Pt–Pt atoms, which are considered to be a mechanism for enhancement of oxygen reduction activity [3]. Fig. 2 shows TEM surface images of PtCo/C and
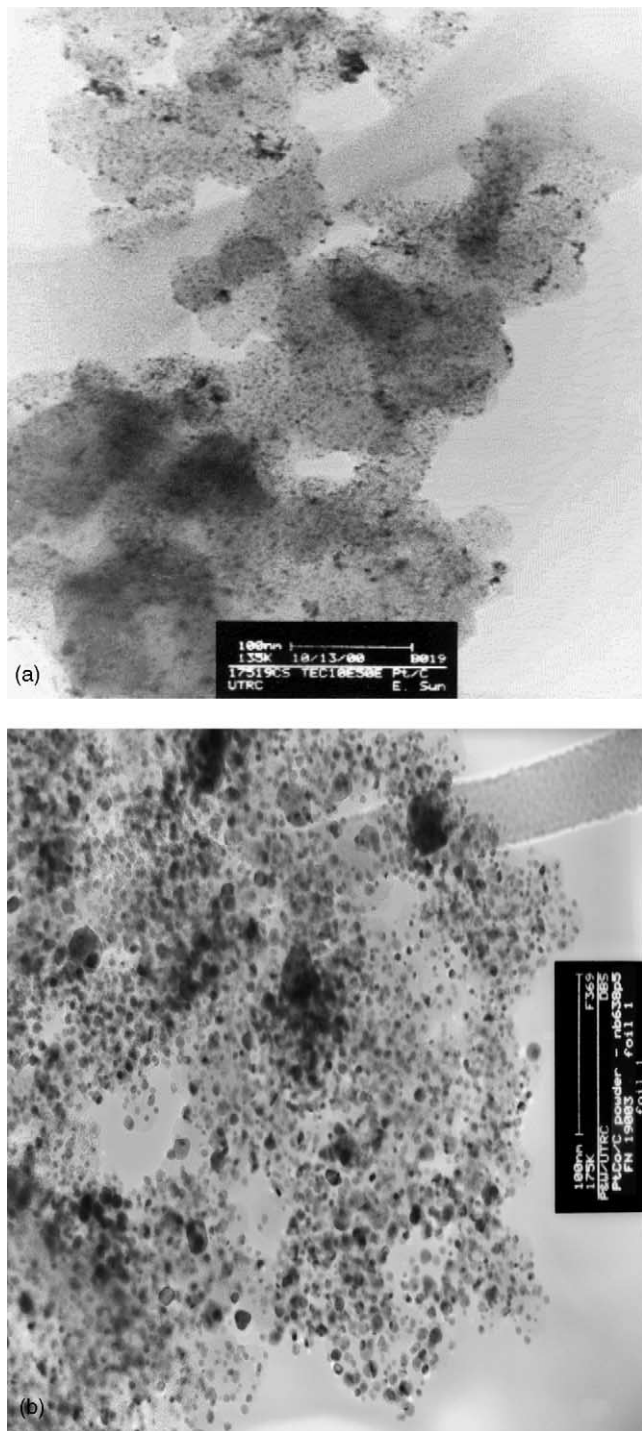

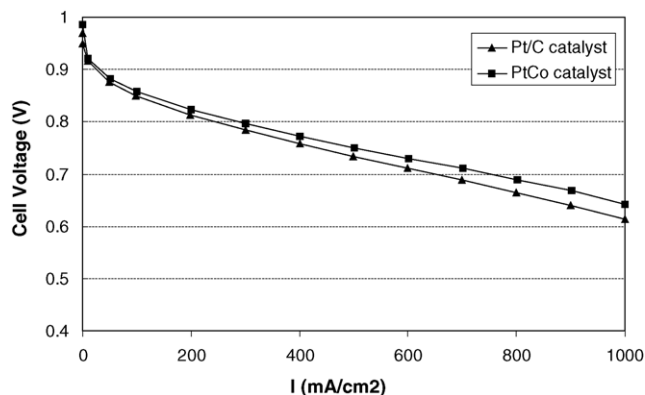Fig. 2. TEM images of (a) Pt/C catalyst (TKK catalyst) and (b) PtCo/C alloy catalyst.

Fig. 3. Initial H_2/air performance curves of MEAs with Pt/C catalyst or PtCo/C catalyst on the cathode at 65 °C. The flow rates of H_2 and air are 500 and 3000 $cm^3 min^{-1}$, respectively.

Pt/C catalysts. A considerable uniformity of catalyst particle is observed for both PtCo/C and Pt/C catalysts. Particle size of PtCo/C catalyst is greater than Pt/C catalyst, which agrees with the XRD results. Composition of PtCo/C catalyst was determined with the inductively couple plasma method and listed in Table 1. The composition of the PtCo/C catalyst was 46.5 wt% Pt and 5.6 wt% Co and an atomic ratio of Pt:Co is 2.5:1 accordingly. The Pt loading of 46.5 wt% in PtCo/C catalyst was comparable to the Pt loading of 48.4 wt% in Pt/C catalyst.

To evaluate a cell performance of Pt/C or PtCo/C catalyst, MEAs with platinum alone or alloy catalyst on the cathode were fabricated and tested in a 5 cm × 5 cm (length × width) subscale cell at 65 °C and 101 kPa (absolute). Fig. 3 presents H_2/air cell performance curves of both MEAs. The cell was held at each current density for 5 min before the cell voltage were record and the polarization curves were taken from high to low current density. As evident in Fig. 3, the cell voltage of PtCo/C MEA was about 10–30 mV greater than that of Pt/C MEA in a current density range of 0.1–1 $A cm^{-2}$, indicating a kinetic enhancement by the PtCo/C catalyst. The kinetic enhancement by the PtCo/C catalyst over Pt/C catalyst generally agrees with the literature [6,12,24]. However, the amount of improvement is slightly lower than the values reported in the literature [6], which, however, is not of major interest in this investigation.

3.2. Durability testing

Pourbaix diagram [18] shows that platinum is unstable at a potential range of 1.0–1.2 V versus SHE and pH of less than or equal to 1. Experimentally, Kinoshita [25] did potential cycling on Pt catalyst supported on carbon in 1 M H_2SO_4 with 1 cycle min^{-1} between 0.05 and 1.25 V. He found the platinum surface area loss of 70% after 3500 cycles due to platinum dissolution. Patterson [26] investigated the effect of potential cycling on a polymer electrolyte membrane fuel cell and he found 50% surface area of platinum was lost after 6500 cycles between 0.87 and 1.2 V with 1 cycle min^{-1}. This

corresponds to a performance loss of about 20 mV. Theoretically, Darling and Meyers developed a mathematical model [27] and predicted that platinum is more vulnerable to dissolution at a transient condition of 0.87 to 1.2 V than at a constant potential of above 1.2 V. As PtCo/C catalyst is getting more interest as a cathode candidate for the application in PEMFCs, concern with the dissolution of cobalt is also rising. Does dissolution of cobalt metal accelerate cell performance degradations? If yes, how? To address these questions, a potential cycling test was conducted by subjecting the cathode side of the cell to a potential square wave of 0.87 and 1.2 V versus RHE with a time step of 30 s at each potential. Cell diagnosis such as H_2/air and H_2/O_2 cell performances were periodically evaluated after every 400 cycles. Membrane resistance and cathode ECA were evaluated at the same time.

Fig. 4 displays H_2/air cell performance of the PtCo/C MEA and the Pt/C MEA after every 400 cycles (H_2/O_2 cell performance curves are not displayed in Fig. 4). It is observed that H_2/air cell performance curve of the Pt/C MEA spread out over cycles with more performance degradation on a longer cycle. In contrast, there was less performance loss on the PtCo/C MEA. To investigate closely, two types of decay rates of each MEA are taken from Fig. 4. One was taken at 0.1 A cm^{-2} of H_2/O_2 curve to reveal a possible effect of

metal dissolution on the oxygen reduction kinetics only. Another rate was determined at 0.5 A cm^{-2} of the H_2/air curve to investigate a possible effect of metal dissolution on both mass transfer resistance and kinetics. Fig. 5 illustrates these decay rates at various cycles. As shown in Fig. 5, most decay rates of PtCo/C MEA except in the 1st 400 cycles were smaller than those of Pt/C MEA. For example, the overall decay rate of PtCo/C MEA at 0.1 A cm^{-2}, H_2/O_2 curve over 2400 cycles was 3.75 μV cycle^{-1}, which was 65% lower than that of Pt/C MEA of 11 μV cycle^{-1} Similarly, the overall decay rate of PtCo/C MEA at 0.5 A cm^{-2} of H_2/air over 2400 cycles was 4.1 μV cycle^{-1}, which was 80% less than 28 μV cycle of Pt/C MEA. These results indicate that dissolution of platinum or cobalt did not impose a more severe impact on cell performances of PtCo/C MEA than Pt/C MEA, especially on the mass transfer resistance related to the membrane conductance. To investigate a possible effect of metal dissolution on membrane conductance, resistances of membrane in both MEAs were determined with a current interruption technique and are summarized in Fig. 6. It is noted that membrane resistances of PtCo/C MEA were constant at the value of 0.088 Ω cm^2 over 2400 potential cycles, while the membrane resistances of Pt/C MEA were in range of 0.086–0.09 Ω cm^2 and increased by 5% over 2400 cycles. This suggests that dissolved cobalt did not dramatically increase the membrane resistance in the PtCo/C MEA by exchanging with protons of Nafion membrane.

To understand the differences in the cell performance and membrane resistance of the PtCo/C MEA and the Pt/C MEA, surface images and cross-section element distribution of platinum or cobalt before and after potential cycling were analyzed with EMPA and are shown in Figs. 7 and 8, respectively. The segments of before cycling were taken from an inactive area of MEA that was covered by Teflon interfacial seals. As shown in Fig. 7(a) and Fig. 8(a), platinum before cycling was uniformly distributed on both cathode and anode segments at a thickness of 15–20 μm. However, distributions of platinum across the MEAs after cycling were different as shown in Fig. 7(b) and Fig. 8(b). A bright and dense platinum band was detected at the interface of cathode and membrane for the PtCo/C MEA, while a bright platinum band was observed in the membrane of the Pt/C MEA after the same cycle testing. These platinum bands were thought to be precipitation of Pt after it dissolved from the cathode when cycling between 0.87 and 1.2 V versus RHE and then diffused into the membrane [26]. It is not fully understood why the precipitation site of platinum in the PtCo/C MEA was different from the Pt/C MEA, however, it is suspected that this could be resulted from a difference in potential profile across the cathode/membrane of the PtCo/C MEA versus Pt/C MEA. It is noted in Fig. 7 that no cobalt element was detected in either the membrane or the anode, suggesting that cobalt did not migrate or precipitate to the membrane/anode during cycling. These results combined with the membrane resistance data in Fig. 6 confirm that dissolution of cobalt did not impose an impact on the membrane conductance of the PtCo/C MEA.
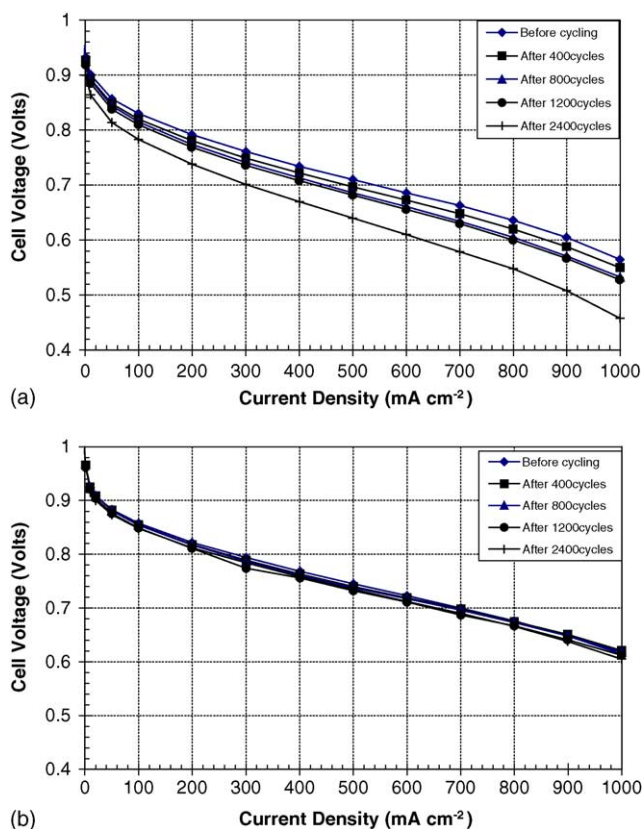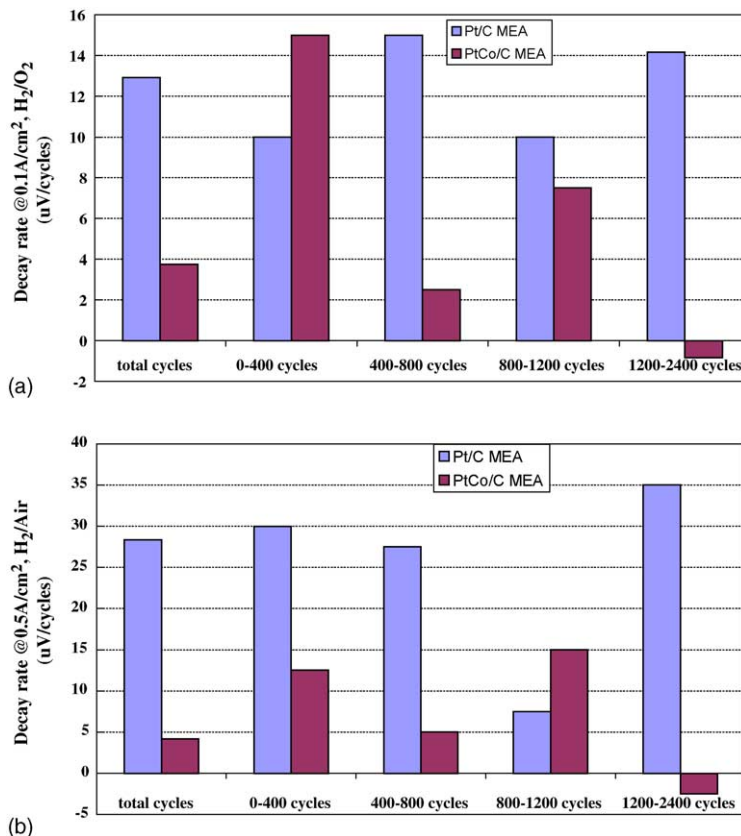

Fig. 4. Cell H_2/air performance curves of (a) Pt/C MEA and (b) PtCo/C MEA after potential cycling for every 400 cycles between 0.87 and 1.2 V vs. RHE. The flow rates of H_2 and air are 500 and 3000 cm^3 min^{-1}, respectively. The cell temperature was 65 °C.

Fig. 5. Decay rates of Pt/C MEA and PtCo/C MEA after potential cycling with H_2/N_2 for various cycles between 0.87 and 1.2 V vs. RHE (a) at 0.1 A cm^{-2}, H_2/O_2 and (b) at 0.5 A cm^{-2}, H_2/air. The flow rates of H_2, air, and O_2 are 500, 3000, and 1000 cm^3 min^{-1}, respectively. The cell temperature was 65 °C. Data were extracted from Fig. 4.

On the other hand, dissolution and precipitation of platinum in the membrane of the Pt/C MEA influences the membrane resistance as shown in Fig. 6. Addition of cobalt to the platinum catalyst altered the site of platinum precipitation in the MEAs and maintained the membrane conductance over 2400 cycles.

Fig. 5(a) also shows that the decay rate at 0.1 A cm^{-2} after the first 400 cycles of H_2/O_2 was 15 μV cycle^{-1} (6 mV in the
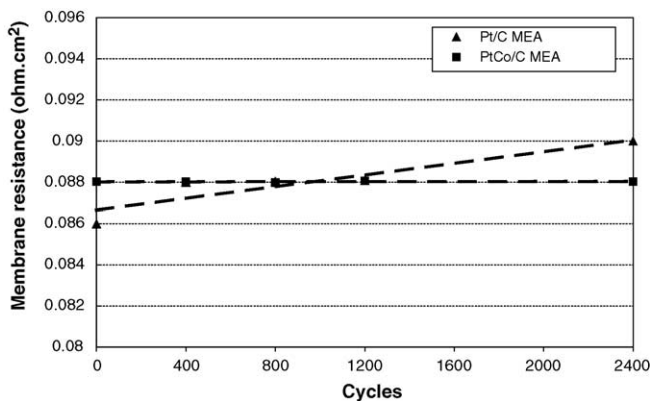

Fig. 6. Membrane resistance as a function of cycle number for PtCo/C and Pt/C MEAs.

total voltage drop) for PtCo/C MEA, about 50% greater than the rate of 10 μV cycle^{-1} (4 mV in the total voltage drop) for Pt/C MEA at the same condition. It is also noted that this decay rate of the PtCo/C MEA was also much higher than those subsequent cycles. To investigate what caused this significant performance decay in the first 400 cycles, two aspects were reviewed: (i) ECAs of the MEAs over potential cycling; this intends to investigate if platinum dissolution in PtCo/C catalyst was more severe than Pt/C catalyst, which might lead to the kinetic loss; (ii) amount of cobalt or platinum dissolution and their impacts on catalyst activity.

Fig. 9 displays cathode ECAs of the PtCo/C MEA and the Pt/C MEA as a function of cycle number. As evident in the figure, ECAs of both PtCo/C MEA and Pt/C MEA decreased with increasing cycling number. It is believed that this was caused by the platinum dissolution and recrystallization during testing. It is also noted that initial ECA of 67 m^2 g^{-1} for the Pt/C MEA was greater than that of 42 m^2 g^{-1} for the PtCo/C MEA, and the rate in ECA decreased in the first 800 cycles was much greater for the Pt/C MEA than for the PtCo/C MEA. This agrees with Darling's model prediction [27] on that a smaller platinum particle size (i.e., larger ECA), a higher platinum dissolution rate, and a greater ECA loss. A cell performance loss can be estimated from the variation of
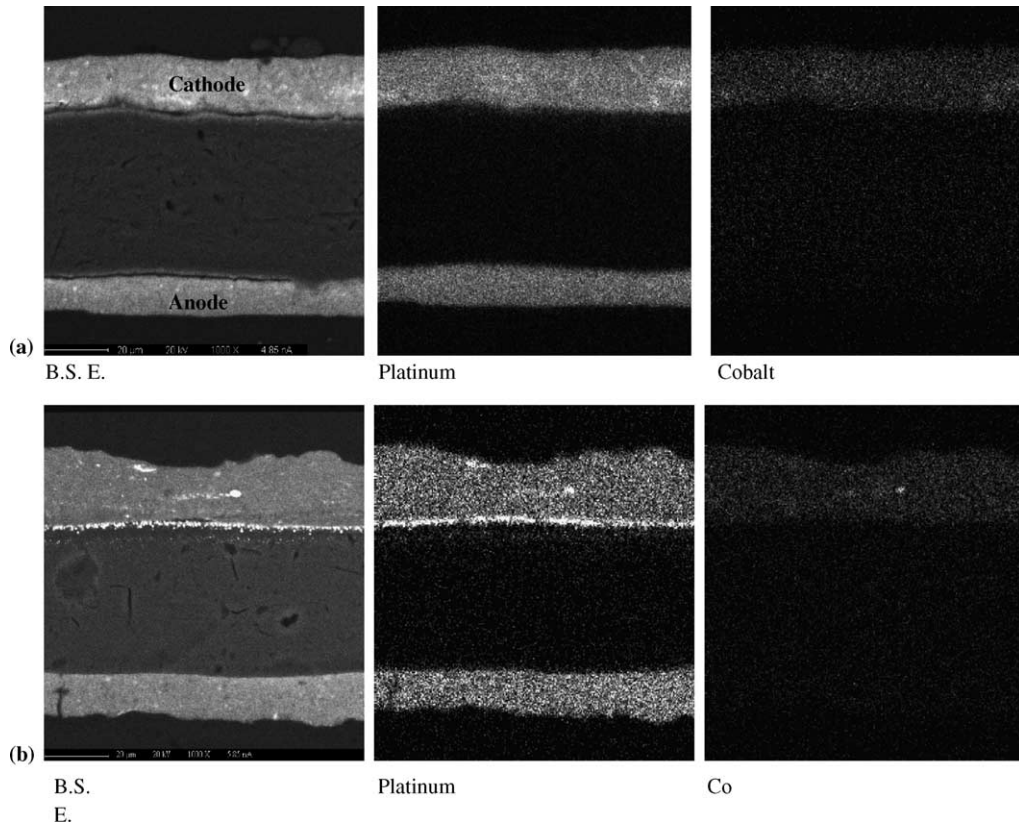
Fig. 7. EMPA images of PtCo MEA (a) before potential cycling and (b) after potential cycling.
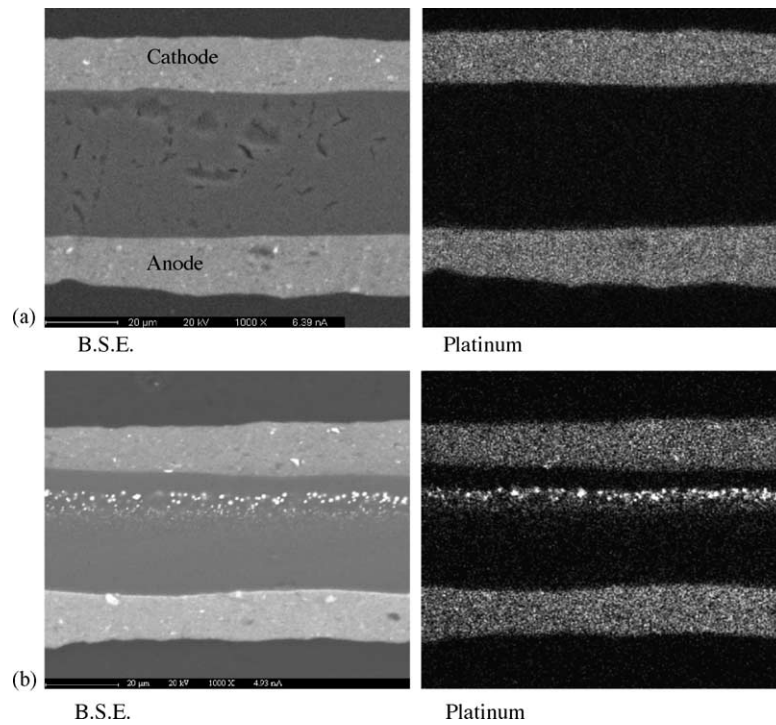

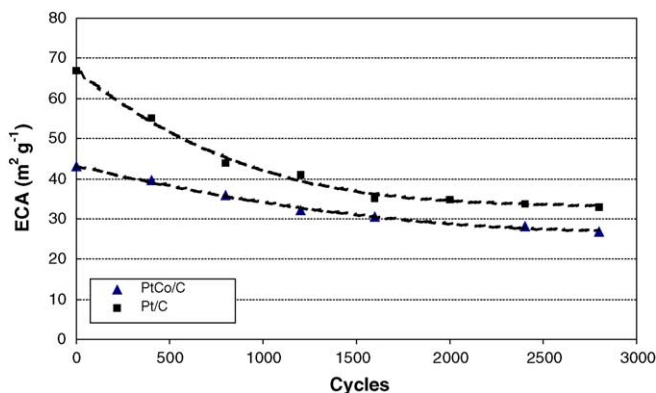Fig. 8. EMPA images of Pt MEA (a) before potential cycling and (b) after potential cycling.

Fig. 9. ECA as a function of cycle numbers of PtCo/C and Pt/C MEAs.

Fig. 10. Cobalt dissolution as a function of cycling number of PtCo/C electrode in a liquid cell of 0.1 M $HClO_4$. The cycling test was conducted at 25 °C.

ECA value by a modified Bulter–Volmer equation [28],

$$\Delta V = 67 \times \log\left(\frac{a_1}{a_2}\right) \tag{1}$$

where ΔV is the cell voltage drop due to a loss of platinum surface area, 67 mV per decade is a Tafel slope at 65 °C and 1 atm (absolute). a_1 and a_2 are the ECAs before and after, respectively. With a variation of ECA of 67 m^2 g^{-1} before and 55 m^2 g^{-1} after 1st 400 cycles for the Pt/C MEA, the cell voltage loss is estimated to be 5.7 mV. Similarly, the performance drop due to ECA loss is calculated to be 2.53 mV for the PtCo/C MEA in the same cycles. Clearly, the performance drop of the PtCo/C MEA was less than that of the Pt/C MEA and this does not explain why there was a higher performance decay rate of the PtCo/C MEA than the Pt/C MEA in the 1st 400 cycles.

To investigate how cobalt or platinum dissolves during potential cycling, a test with the same protocol as shown above was conducted on a Teflon-bonded electrode of the PtCo catalyst in a liquid cell of 0.1 M $HClO_4$ acid and with a three-electrode system at 25 °C. In the three-electrode system, the PtCo/C catalyst bonded with Teflon was used as a working electrode, a platinum wire as a counter, and H_2/Pt as a reference electrode. The Pt loading of the catalyst electrode was 0.1 mg cm^{-2} and the geometric area of electrode was 1 cm^2. The perchloric acid electrolyte was periodically taken out from the liquid cell for Co^{2+} and Pt^{2+} concentration analysis (with ICP method) after each 400 cycles and new $HClO_4$ acid was placed in the liquid cell for the next testing cycle. Fig. 10 presents the Co^{2+} concentration as a function of cycling number. It is noted that 13.9 mol% cobalt dissolved in the 1st 400 cycles. The amount of cobalt dissolution was reduced subsequently and leveled off to approximately 6% after 800 cycles. This result was coincidental with a high performance loss in the 1st 400 cycles and lower loss in subsequent cycles, as shown Fig. 5(a). ICP analysis results also indicated that the amount of platinum ion was not sufficient for detection from the acid solution at each 400 cycles, indicating that amount of platinum dissolution was much smaller than cobalt. These results suggest that the higher performance loss of PtCo/C MEA
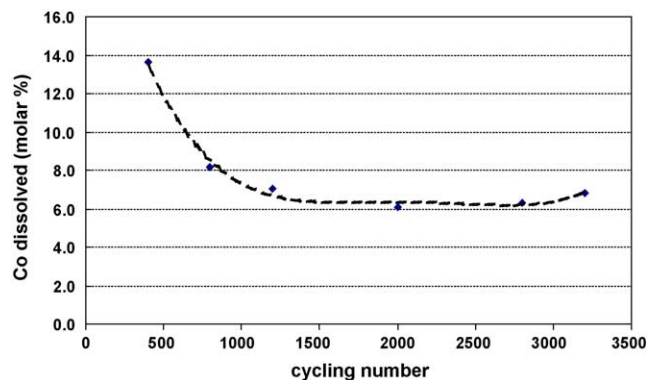
at 1st 400 cycles might be related to a significant amount of cobalt dissolution instead of platinum dissolution. To further confirm the loss of cobalt from the PtCo/C alloy, XRD analysis was conducted to determine the platinum lattice parameter of the alloy samples before any cycle and after 2400 cycles and the results are illustrated in Table 2. It is seen that the lattice parameter of PtCo/C catalyst increased from 0.382 nm of before cycling to 0.387 nm of after cycling, which led the alloy more platinum like in composition (lattice parameter of platinum is 0.392 nm). The liquid cell data and the XRD result confirm that cobalt dissolution occurs over potential cycles and the alloy crystal structure altered as well.

To determine how the cobalt dissolution affects the oxygen reduction kinetics, variation of intrinsic activity, i.e., mass activity and specific activity, for both PtCo/C and Pt/C catalysts over cycles were investigated. The mass activity (A g^{-1} Pt) was obtained from a current density at 0.9 V of H_2/O_2 performance curve and specific activity (A m^{-2} Pt) was calculated from the ratio of mass activity to the ECA values in the corresponding cycles. Fig. 11 displays the results. As evident in Fig. 11, the mass activities of PtCo/C and Pt/C decreased over cycles and no profound loss in mass activity of PtCo/C over Pt/C catalyst was found over 2400 cycles. However, an opposite variation in the specific activity of PtCo/C and Pt/C catalyst was observed in the 1st 400 cycles, i.e., the specific activity of PtCo/C decreased about 5% from 4.60 to 4.36 A m^{-2} Pt, while Pt/C increased about 10% from 1.46 to 1.60 A m^{-2} Pt. The trend of specific activity for Pt/C catalyst over 400 cycles agrees well with Kinoshita's result [29] in that the specific activity increases with increasing platinum particle size at longer cycles. The opposite trend of specific

Table 2
Lattice parameters of PtCo catalyst before and after potential cycling

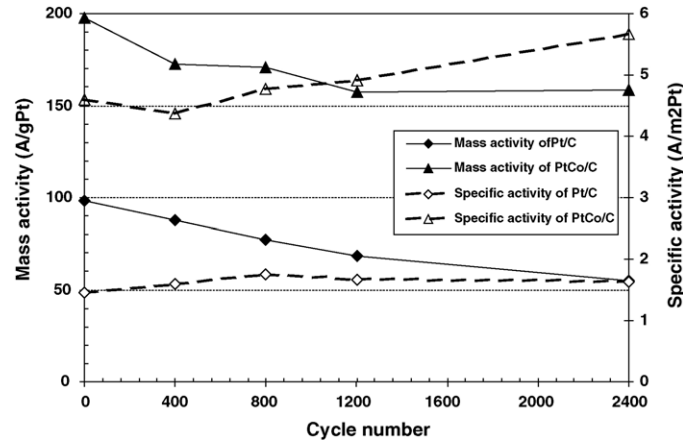| Catalyst	Lattice parameter (nm)
Pt[a]	0.392
Co[a]	0.355
PtCo/C (before cycled)	0.382
PtCo/C (after cycled)	0.387

[a] Data were taken from Ref. [30].

Fig. 11. Mass activity and specific activity of PtCo/C and Pt/C catalyst over cycles. Data were extracted from the current density at 0.9 V of H_2/O_2 curves after potential cycles. The flow rates of H_2 and O_2 were 500 and 1000 $cm^3 min^{-1}$, respectively. The cell temperature was 65 °C.

activity for PtCo/C catalyst suggests that a factor in addition to the particle size predominantly contributes to the activity loss. Based on the liquid cell investigation and XRD results, it is reasonable to induce that cobalt dissolution leads to the loss of specific activity of PtCo/C catalyst in the 1st 400 cycles. It is also noted in Fig. 11 that the specific activities of PtCo/C catalyst after 400 cycles increases with cycles, a same trend as in Kinoshita's result. This suggests that platinum particle size in addition to the cobalt dissolution contributes to the variation of specific activity after 400 cycles.

To determine what really caused the more substantial performance loss of Pt/C MEA over the PtCo/C MEA for 2400 cycles, cell voltage drops at various cycles were calculated from the corresponding ECA values (presented in Fig. 9) using the Eq. (1) and are displayed in Fig. 12. The actual cell voltage drops were presented in the figure as well for comparison. The actual cell voltages were taken at 0.1 A cm^{-2} of H_2/O_2 curves after potential cycles and the variation of cell voltage assumedly reflects only the kinetic loss of catalyst.
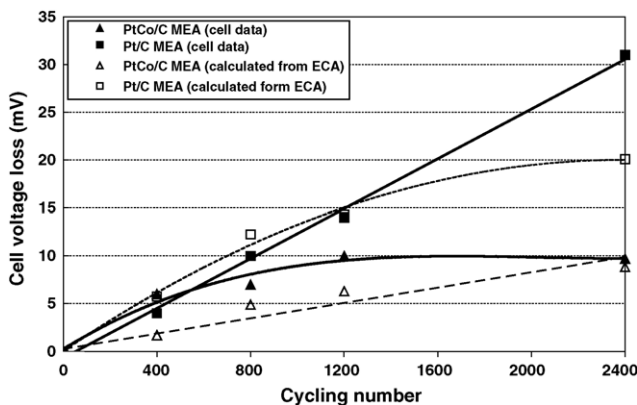

Fig. 12. Comparison of cell voltage losses of Pt/C and PtCo/C MEAs estimated from the ECA values with the actual cell data. The actual cell voltages were taken at 0.1 A cm^{-2} of H_2/O_2 curves after potential cycles. The flow rates of H_2 and O_2 were 500 and 1000 $cm^3 min^{-1}$, respectively. The cell temperature was 65 °C.

As evident in Fig. 12, the cell voltage drops of Pt/C MEA estimated from values of ECA loss is agreeable to the cell data up to 1200 cycles, indicating that the performance loss of Pt/C MEA was mainly resulted from the ECA loss. This result generally agrees with Patterson's result and the ECA loss was mainly due to the platinum dissolution and recrystallization. As illustrated by Kinoshita [29], the lower the ECA, i.e, the greater the platinum particle size (when greater than 3 nm), then the smaller the mass activity, i.e, the lower the kinetics, and eventually the lower the cell voltage. The cell voltage drop of Pt/C MEA after 1200 cycles estimated from the ECA loss was greater than the cell data, indicating that other factors in addition to the ECA loss contributed to the cell performance loss. Based on the EMPA analysis, it was suspected that the platinum precipitation in the membrane was a possible factor for this because increased membrane resistances were observed in the corresponding cycles. On the other hand, the cell voltage drops of the PtCo/C MEA among 2400 cycles estimated from the ECA values was disparate from the actual cell data up to 1200 cycles, indicating that the ECA loss was not the only factor for the performance loss in the PtCo/C MEA. Based on the experimental data in Fig. 10 and the corresponding analysis, it is induced that the activity loss due to cobalt dissolution is a substantial factor that contributes to the performance loss of the PtCo/C MEA.

4. Conclusions

The durability of the PtCo/C cathode catalyst has been evaluated in a dynamic fuel cell environment with continuous water fluxing on the cathode. A potential cycling test between 0.87 and 1.2 V versus RHE was applied to the system to illustrate how cobalt or platinum dissolution might affect the cell performance. The results indicate that cobalt dissolution neither detrimentally reduces the cell voltage nor dramatically affects the membrane conductance. Cell performance enhancement by PtCo/C over Pt/C catalyst has been

sustained over 2400 cycles. Potential cycle testing has been shown to accelerate cobalt dissolution as indicated in a substantial loss of catalyst activity in the 1st 400 potential cycles. The performance losses of the Pt/C MEA over 1200 cycles were mainly resulted from the ECA loss due to the platinum recrystallization, while the performance losses of the PtCo/C MEA were resulted from the activity loss due to the cobalt dissolution as well as the ECA loss.

Acknowledgements

References

[1] D. Thompsett, in: W. Vielstich, A. Lamm, H.A. Gasteiger (Eds.), Handbook of Fuel Cells: Fundamentals, Technology, and Applications, vol. 3, John Wiley & Sons, New York, 2003 (Chapter 37).

[2] H.A. Gasteiger, M. Mathias, Abstracts of 202nd The Electrochemical Society Meeting Abstract 815, Salt Lake City, Utah, 2002.

[3] D.A. Landsman, F.J. Luczak, In: W. Vielstich, A. Lamm, H.A. Gasteiger (Eds.), Handbook of Fuel Cells: Fundamentals, Technology, and Applications, vol. 4, John Wiley & Sons, New York, 2003 (Chapter 65).

[4] N.M. Markovic, B.N. Grgur, P.N. Ross, J. Phys. Chem. B 101 (1997) 5405.

[5] M. Watanabe, K. Tsurumi, T. Mizukami, T. Nakamura, P. Stonehart, J. Electrochem. Soc. 141 (1994) 2659.

[6] S. Mukerjee, S. Srinivasan, J. Electroanal. Chem. 357 (1993) 201.

[7] A.J. Appleby, Energy 11 (1986) 13.

[8] J.C. Huang, R.K. Sen, E. Yeager, J. Electrochem. Soc. 126 (1979) 786.

[9] V. Jalan, E.J. Taylor, J. Electrochem. Soc. 130 (1983) 2299.

[10] V. Stamenkovic, T.J. Schmidt, P.N. Ross, N.M. Markovic, J. Electroanal. Chem. 554 (2003) 191.

[11] V. Stamenkovic, T.J. Schmidt, P.N. Ross, N.M. Markovic, J. Phys. Chem. B 106 (2002) 11970.

[12] T. Toda, H. Igarashi, H. Uchida, M. Watanabe, J. Electrochem. Soc. 146 (1999) 3750.

[13] J. Dt-Pierre, D.P. Wilkinson, S. Knights, M.L. Bos, J. New Mater. Electrochem. Syst. 3 (2000) 99.

[14] T.R. Ralph, M.P. Hogarth, Platinum Met. Rev. 46 (2002) 3.

[15] T. Okada, in: W. Vielstich, A. Lamm, H.A. Gasteiger (Eds.), Handbook of Fuel Cells: Fundamentals, Technology, and Applications, vol. 3, John Wiley & Sons, New York, 2003 (Chapter 37).

[16] T. Okada, Y. Ayato, M. Yuasa, I. Sekine, J. Phys. Chem. B 103 (1999) 3315.

[17] T. Okada, G. Xie, Electrochim. Acta 43 (1998) 3741.

[18] M. Pourbaix, Altas of Electrochemical Equilibrium in Aqueous Solutions, Pergamon Press, New York, 1966.

[19] T. Okada, Y. Ayato, H. Satou, M. Yuasa, I. Sekine, J. Phys. Chem. B 105 (2001) 6980.

[20] US Patents 5,189,005 (1993); 5,593,934 (1997).

[21] US Patents 5,013,618 (1991); 4,880,711 (1989); 4,447,506 (1984).

[22] US Patent 5,700,595 (1997).

[23] D. Wheeler, J. Yi, R. Fredley, D. Yang, T. Patterson, L. VanDine, J. New Mater. Electrochem. Syst. 4 (2001) 233.

[24] U.A. Paulus, A. Wokaun, G.G. Scherer, T.J. Schmidt, V. Stamenkovic, B. Radmilovic, N.M. Markovic, P.N. Ross, J. Phys. Chem. B 106 (2002) 4181.

[25] K. Kinoshita, J. Electroanal. Chem. Interfacial Electrochem. 48 (1973) 157.

[26] T. Patterson, Fuel cell technology: opportunities and challenges, in: AIChE Spring National Meeting Proceedings, 2002, p. 313.

[27] R. Darling, J. Meyers, J. Electrochem. Soc. 150 (2003) 1523.

[28] G. Prentice, Electrochemical Engineering Principles, Prentice Hall Inc., New Jersey, 1991.

[29] K. Kinoshita, Electrochemical Oxygen Technology, John Wiley & Sons Inc., New York, 1992, pp. 48.

[30] J.R. Anderson, Structure of Metallic Catalysts, Academic Press, New York, 1975.